Equilibrium phase diagrams for the elongation of epitaxial quantum dots into hut-shaped clusters and quantum wires

I. Daruka,[1,*] C. Grossauer,[1] G. Springholz,[1] and J. Tersoff[2]

[1]*Johannes Kepler University, Institute of Semiconductor and Solid State Physics, Altenbergerstrasse 69, A-4040 Linz, Austria*

[2]*IBM T. J. Watson Research Center, 1101 Kitchawan Road, Yorktown Heights, New York 10598, USA*

(Received 28 March 2014; revised manuscript received 21 May 2014; published 20 June 2014)

The formation of self-assembled nanoislands is an important and much-studied feature of strained layer epitaxial growth. The varied island shapes such as pyramids, hut clusters, and elongated nanowires are considered promising building blocks for nanodevice applications. However, even some basic aspects of their growth and energetics are not fully understood. In particular, for Ge on Si (001), it has been recently proposed that the low surface energy of {105} facets renders the (001) surface unstable even neglecting bulk strain energy. Here we calculate how the competition between strain, surface energies, and edge energies determines the equilibrium shapes of epitaxial islands. In particular, we examine the novel regimes that can arise when the (001) surface becomes unstable against faceting. Our calculations thus provide an overview of the equilibrium island shapes as a natural starting point for consideration of possible kinetic effects.

DOI: 10.1103/PhysRevB.89.235427 PACS number(s): 68.55.ag, 68.55.J−

I. INTRODUCTION

Heteroepitaxial growth offers a wealth of self-assembled nanostructure shapes. The simplest shapes are square-base pyramids [1–3] and rectangular-base prisms, often called "hut clusters" [4,5]. Despite extensive experimental [1–6] and theoretical [7–9] studies, the growth mechanisms are still not completely understood. In addition, recent studies have demonstrated the formation of very long narrow islands [10–13], i.e., in-plane nanowires, with rather promising quantum-transport applications [14]. Figure 1 shows the salient self-assembled island morphologies observed in Ge on Si (001), the prototypical system for such studies. Throughout this paper we have Ge/Si in mind, while noting that III-V systems show behavior very similar to Ge/Si [15–17].

Since the earliest reports of faceted Ge "quantum dots" [4], the elongated island shapes have posed an outstanding puzzle. It is known that elastic relaxation can drive elongation in quasi-2D systems, but not in 3D prismatic islands [18]. Therefore the elongation has generally been attributed to kinetic effects [19,20]. Indeed, there are sound theoretical arguments to suggest that the behavior could be controlled by kinetics more than by thermodynamics [21]. In any case, an understanding of the thermodynamics and possible equilibrium shapes seems a natural starting point, and that is our focus here.

In understanding the formation and growth of faceted heteroepitaxial nanostructures, the excess surface energy (ESE) plays a central role. The ESE of a faceted island can be defined as the difference between the total surface energy per substrate surface area of the system in the presence of the island, and without it, i.e., when only a wetting layer is present. Until recently, it was universally assumed that the ESE is positive; i.e., island formation increases the surface energy [7,22]. However, recent *ab initio* calculations for idealized zero-temperature geometries have suggested a negative ESE of the Ge {105} facets under epitaxial compression, relative to the (001) wetting layer orientation [23–25]. Indeed, equilibrium models including a negative ESE were used to explain the formation and growth of pyramidal islands [9] and also the recently observed Ge/Si nanowires [12] and nanoripples [26]. In this scenario the edge energies, which are usually neglected, take on a central role. Unfortunately little is known about the structure and energetics of facet edges at the growth temperature.

If, as those calculations suggest, the surface energy actually decreases with island formation, this could require a wholesale revision of our understanding of these systems. However, many uncertainties remain. The *ab initio* calculations involve idealized geometries that tend to systematically overestimate the (001) free energy, and thus underestimate the surface energy cost for island formation. The most obvious issue is that most *ab initio* surface-energy calculations do not consider the real $N \times M$ missing-dimer reconstruction of Ge on Si (001), which is very complex [27] and has strain fields extending deep into the substrate. Also, intermixing between the Si substrate and the Ge wetting layer tends to lower the (001) free energy via site-specific segregation [28], among other effects. Finally we note that zero-temperature calculations may significantly overestimate the (001) free energy and underestimate the ESE by neglecting thermal fluctuations, which appear to roughen the (001) surface but not the (105) [29]. Thus there are reasons to think that the (001) might be more stable relative to {105} than idealized zero-temperature calculations suggest.

Given the many uncertainties regarding even the most basic thermodynamic parameters such as surface energies [8,9,12] and edge energies [12,30,31], and even the sign of the ESE, there is a need for a broad overview of the island energetics, in order to understand how these energies determine the equilibrium shape. While the real system may be far from equilibrium, an understanding of the equilibrium shape is a natural starting point for analyzing the competition between thermodynamics and kinetics in determining the actual morphology. Along these lines, this work was particularly motivated by the recent experimental and theoretical investigations of nanowire formation in the Ge/Si(001) heteroepitaxial system [12,13] and by the unsettled issues regarding the formation and growth of these nanostructures [8,9,12,30].

*Istvan.Daruka@jku.at

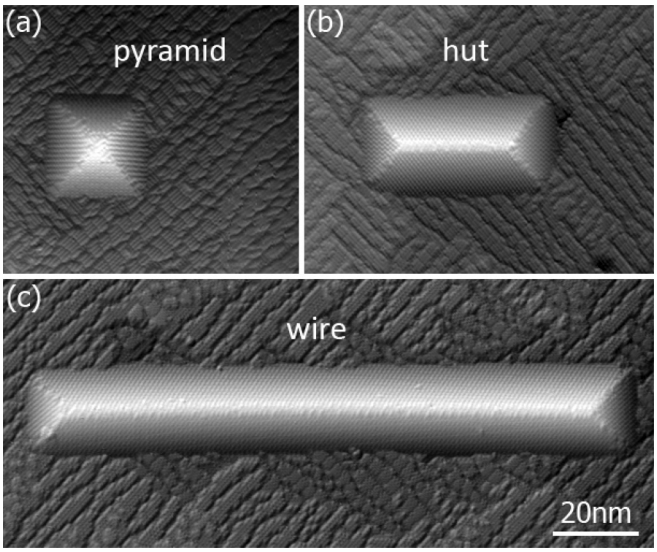

FIG. 1. Scanning tunneling microscopy images of (a) pyramids, (b) elongated hut clusters, and (c) wires formed in Ge heteroepitaxy on Si (001) at 550 °C, at a coverage of approximately 5 ML. All islands display the same {105} type of facets, while exhibiting rather different geometric aspect ratios of $L/B = 1, 2$, and 7 from (a) to (c), respectively. All images are at the same scale.

In order to give a comprehensive characterization of the possible morphologies, we investigate the equilibrium shapes and energetics of rectangular-based islands over a wide range of material parameters. Beyond clarifying the role of the interplay of surface, edge, and elastic energy contributions, our findings could also provide potential guidance for experimentalists in searching for nanowires with optimal structural properties for quantum-transport experiments [14].

II. ISLAND ENERGETICS

First, we derive an analytic approximation for the total energy of an island with a rectangular base of length L and width B formed on top of a planar wetting layer. We assume that the island is composed of four equivalent facets inclined relative to the substrate, as shown in Fig. 2. The total energy is taken to be the sum of the extra surface energy, the edge energy contributions, and the elastic relaxation energy contribution.

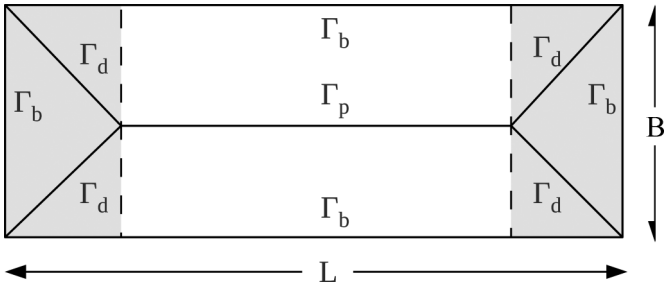

FIG. 2. Top view of an elongated hut cluster with length L and width B. The labels for the respective edge energies are indicated. To calculate the elastic relaxation energy, we approximate the energy density in the shaded end areas separated by dashed lines as having the value ρ_p calculated for square-based pyramids. The unshaded middle part of the island is approximated as a section of an infinite wire, with an elastic relaxation energy contribution ρ_w.

Even within the simple geometry of Fig. 2, there are several inequivalent edges. As a compromise between generality and simplicity, we assign zero energy to the concave edges at the base, while distinguishing between the diagonal edges with energy Γ_d, and the top edge parallel to the base edge with energy Γ_p, as indicated in Fig. 2.

The total energy of an island formed on top of a planar wetting layer can be written as

$$E_{\text{tot}} = E_{\text{strain}} + E_{\text{surface}} + E_{\text{edge}}, \tag{1}$$

where

$$E_{\text{strain}} = \tilde{V}\rho_r, \tag{2}$$

$$E_{\text{surface}} = \tilde{V}^{2/3}\Delta\gamma\left(\frac{1}{b} + \frac{b^2}{3}\right), \tag{3}$$

$$E_{\text{edge}} = \tilde{V}^{1/3}\Gamma_p\left(\frac{1}{b^2} + \chi b\right) \tag{4}$$

correspond to the bulk strain energy, surface energy, and edge energy contributions, respectively, and the total energy is calculated relative to the same amount of material distributed as a planar wetting layer (i.e., no strain relaxation or ESE effects). In the above equations $\tilde{V} = 4V/\tan\alpha$ is the scaled

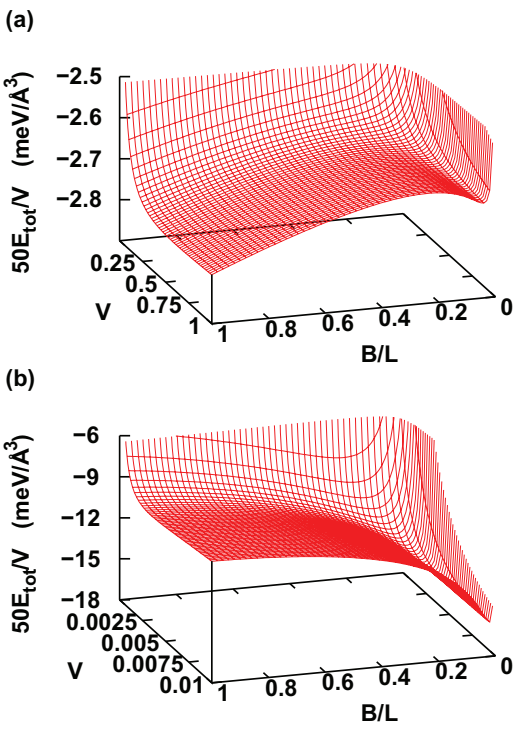

FIG. 3. (Color online) Total island energy per volume ($50E_{\text{tot}}/V$, meV/Å^3) for two different values of the excess surface energy $\Delta\gamma$ plotted as a function of island volume V [in units of (100 nm)^3] and island aspect ratio B/L. (a) At $\Delta\gamma = -0.8$ meV/Å^2, the pyramidal shape is preferred; (b) at $\Delta\gamma = -4.5$ meV/Å^2, elongated huts/wires are favored. The island aspect ratio $B/L = 1$ corresponds to square-based pyramids, and $B/L = 0$ corresponds to infinitely long wires.

island volume with α being the facet inclination with respect to the substrate, and $V = (3L - B)B^2 \tan\alpha/12$ being the island volume. $b = B/\tilde{V}^{1/3}$ is the scaled island base width, which can be related to the geometrical aspect ratio L/B via $L/B = b^{-3} + 1/3$. $\Delta\gamma = \gamma_\alpha \sec\alpha - \gamma_{WL}$ is the excess surface energy (ESE) discussed in the introduction, with γ_α being the side facet surface energy of the island, and γ_{WL} the surface energy of the wetting layer. Furthermore, $\chi = 2(\phi g_r - 1/3)$ with $g_r = \Gamma_d/\Gamma_p$ being the edge energy ratio between the diagonal and top edges, and $\phi = \sqrt{1+\cos^2\alpha}/\cos\alpha$ a geometrical factor. We note that due to the factor $\sec\alpha$ in the above formula of the ESE $\Delta\gamma$, the surface energy of the islands' side facet γ_α would need to be lower than the surface energy of the wetting layer γ_{WL} by at least a factor of $\cos\alpha$ to arrive at a negative ESE.

Finally, since we do not need a highly accurate determination of the strain energy here, we treat the elastic relaxation term ρ_r as follows. We divide the elastic relaxation energy of the elongated hut clusters into contributions from the two ends and the middle section. The two ends of an elongated island are approximated as having the same combined elastic relaxation energy as the corresponding pyramid. The middle section is approximated as having the same elastic relaxation energy as a section of the same length from an infinite wire. This is indicated schematically in Fig. 2. In this way we only need calculations of the elastic relaxation energy for pyramids and infinite wires [32]. This treatment omits any contributions arising from the edge-edge interactions [33]. Therefore, one can write

$$\rho_r = \rho_w + \tfrac{2}{3}(\rho_p - \rho_w)b^3, \tag{5}$$

where ρ_p and ρ_w are the elastic relaxation energies per unit volume for pyramids and wires, respectively.

For any give set of parameters (including volume), the equilibrium island shape was obtained by minimizing Eq. (1) numerically with respect to the scaled island base width b.

III. PHASE DIAGRAMS FOR ISLAND SHAPE

In this section we present the results of our calculations as three sets of island-shape phase diagrams. In this way we provide a concise and rather generic characterization of the possible morphologies. The results demonstrate how the interplay of excess surface energy (ESE) and the other model parameters contributes to the occurrence of elongated morphologies.

Our model for the island energy has the following parameters: α, ρ_w, ρ_p, $\Delta\gamma$, Γ_p, and g_r. To focus on the key features, we

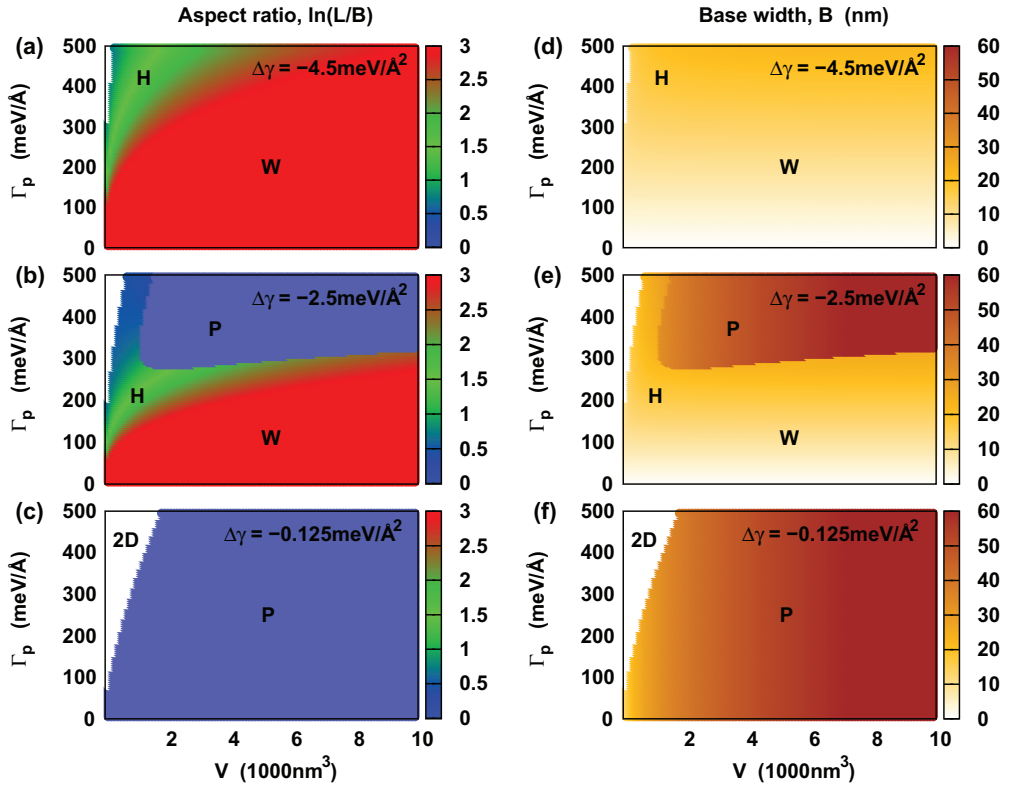

FIG. 4. (Color online) (a)–(c) Shape phase diagrams for different values of excess surface energy $\Delta\gamma$, as a function of island volume V and edge energy Γ_p. Values of $\Delta\gamma$ are (a) -4.5 meV/Å^2, (b) -2.5 meV/Å^2, and (c) -0.125 meV/Å^2. The colors correspond to the logarithm of the island's aspect ratio $\ln(L/B)$. In particular, the blue color corresponds to a pyramidal island shape [P; $\ln(L/B) = 0$]; the green color represents moderate elongation, i.e. "hut clusters" (H); and the red color corresponds to very elongated islands, i.e., wires (W). The white regions correspond to regimes where planar growth with no island formation is preferred. We note that there are three distinct phases separated by first-order transitions: planar "2D"; pyramids "P"; and elongated islands "H" and "W" (which are regions of the same phase, distinguished somewhat arbitrarily by aspect ratio). (d)–(f) Corresponding island base widths B (in nm) plotted as a function of island volume V and edge energy Γ_p.

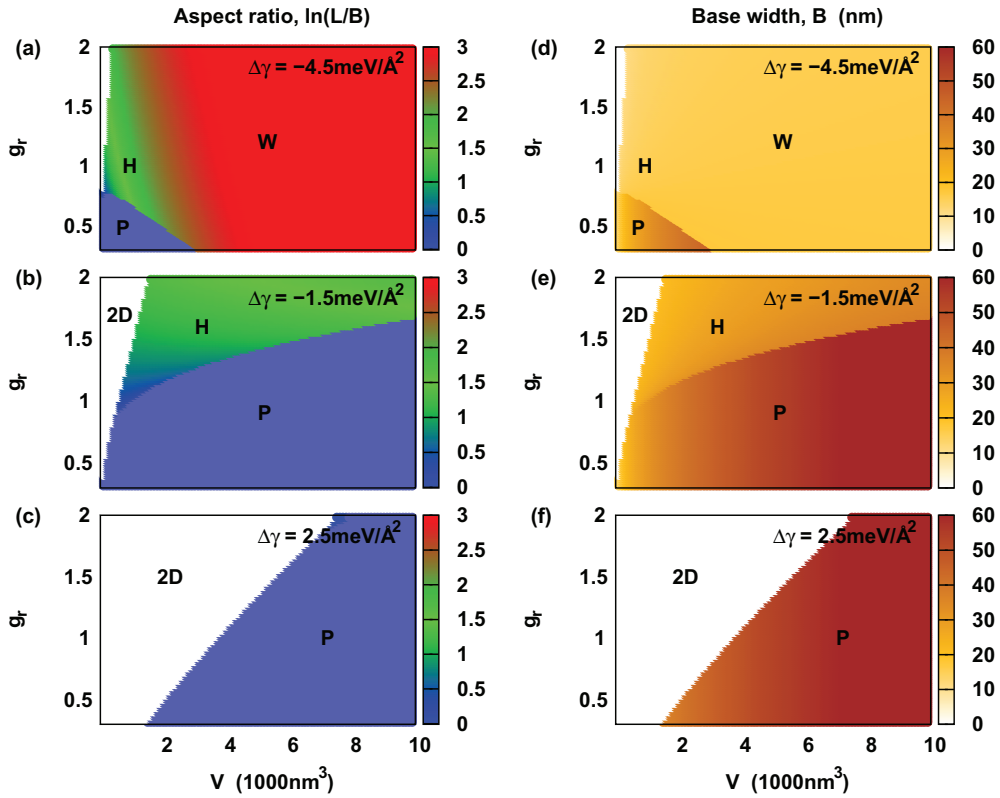

FIG. 5. (Color online) (a)–(c) Shape phase diagrams at three different values of excess surface energy $\Delta\gamma$, as a function of island volume V and edge energy ratio g_r. Values of $\Delta\gamma$ are (a) -4.5 meV/Å^2, (b) -1.5 meV/Å^2, and (c) 2.5 meV/Å^2. The colors correspond to the logarithm of the island's aspect ratio $\ln(L/B)$. In particular, the blue color corresponds to a pyramidal island shape [P; $\ln(L/B) = 0$]; the green color represents moderate elongation, i.e., "hut clusters" (H); and the red color corresponds to very elongated islands, i.e., wires (W). The white regions correspond to regimes where planar growth with no island formation is preferred. We note that there are three distinct phases separated by first-order transitions: planar "2D"; pyramids "P"; and elongated islands "H" and "W" (which are regions of the same phase, distinguished somewhat arbitrarily by aspect ratio). (d)–(f) Corresponding island base widths B (in nm) plotted as a function of island volume V and edge energy ratio g_r.

use the Ge/Si(001) system as a reference and thus, we fix the facet angle $\alpha = 11.3^\circ$, corresponding to the {105} faceted Ge island geometry on a {001} substrate (see Fig. 1), and we take $\rho_p/\rho_w = 1.137$ as suggested by finite-element calculations for Ge on Si (001) [32]. We take as default values for the edge energies $\Gamma_p = \Gamma_d = 370$ meV/Å [26], i.e., ratio $g_r = 1$, and take $\rho_w = 0.2585$ meV/Å^3 [12]. Then we vary one parameter at a time to study their effects.

Figure 3 shows the island energy landscape as a function of the island volume V and aspect ratio B/L. One can find basically two different scenarios. For higher values of ESE $\Delta\gamma$, the pyramidal shape ($B/L = 1$) dominates [Fig. 3(a)], while below a certain ESE, elongated island shapes ($B/L \ll 1$) are preferred [Fig. 3(b)].

Next, we use Eq. (1) to determine the minimum-energy island shapes as a function of the key physical parameters. In this way we created several shape phase diagrams, each describing the equilibrium island shape as a function of the island volume and one parameter: (i) the edge energy Γ_p (taking both types of edge to have the same energy) in Fig. 4; (ii) the ratio g_r between energies of diagonal and parallel edges in Fig. 5; and (iii) the wire elastic relaxation energy density ρ_w in Fig. 6. These plots of equilibrium island shape also serve as phase diagrams, where discontinuous changes in shape indicate thermodynamic transitions between pyramidal islands, elongated islands, and planar geometries having only a 2D wetting layer.

As we focus our investigations on the novel effects of the negative ESE, each set consists of three phase diagrams corresponding to three different values of the ESE, starting from lower (very negative) values of $\Delta\gamma$ towards higher values.

The first set of plots [Figs. 4(a)–4(c), left column] describes the favored island shapes as a function of the island volume V and the edge energy, assuming $\Gamma_d = \Gamma_p$. For very negative values of $\Delta\gamma$ elongated island shapes are preferred [Fig. 4(a)]. At moderately negative values of $\Delta\gamma$ the pyramidal shape also appears in the phase diagram, with a first-order phase boundary line between the pyramidal and elongated shapes [Fig. 4(b)]. At even higher values of $\Delta\gamma$, only pyramids appear in the investigated range of parameters [Fig. 4(c)].

The second set of phase diagrams shown in Figs. 5(a)–5(c) describes the favored island shapes as a function of the island volume V and the edge energy ratio g_r. We find that for very negative values of $\Delta\gamma$ and not too small values of g_r elongated wires are favored, but there is also a small parameter region confined to small volumes and small g_r

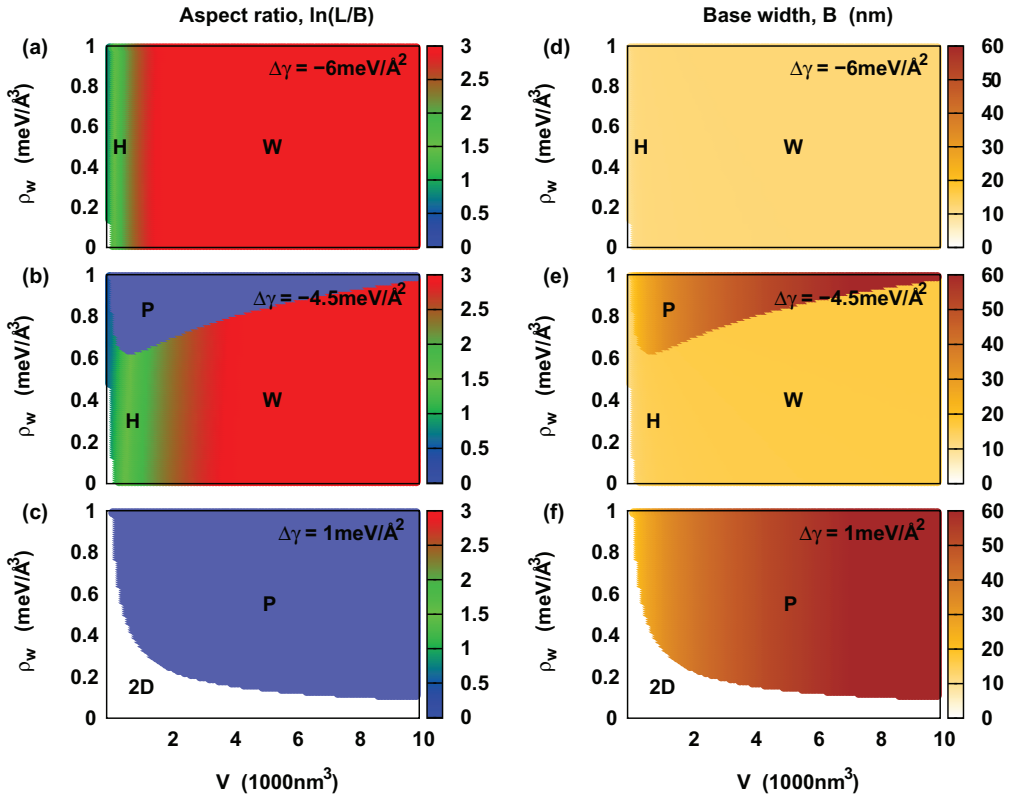

FIG. 6. (Color online) (a)–(c) Shape phase diagrams at three different values of excess surface energy $\Delta\gamma$, as a function of island volume V and elastic relaxation energy density ρ_w. Values of $\Delta\gamma$ are (a) -6.0 meV/Å^2, (b) -4.5 meV/Å^2, and (c) 1.0 meV/Å^2. The colors correspond to the logarithm of the island's aspect ratio $\ln(L/B)$. In particular, the blue color corresponds to a pyramidal island shape [P; $\ln(L/B) = 0$]; the green color represents moderate elongation, i.e. "hut clusters" (H); and the red color corresponds to very elongated islands, i.e., wires (W). The white regions correspond to regimes where planar growth with no island formation is preferred. We note that there are three distinct phases separated by first-order transitions: planar "2D"; pyramids "P"; and elongated islands "H" and "W" (which are regions of the same phase, distinguished somewhat arbitrarily by aspect ratio). (d)–(f) Corresponding island base widths B (in nm) plotted as a function of island volume V and elastic relaxation energy density ρ_w.

values where pyramids are preferred. This is because for small g_r values the diagonal edges have significantly lower energy per unit length than the top edge and thus, the edge energy costs for island elongation would be higher. As $\Delta\gamma$ increases, the pyramidal phase dominates more and more [Fig. 5(b)]. Above a certain value of $\Delta\gamma$, only pyramids form in the investigated range of parameters [Fig. 5(c)].

The third set of phase diagrams shown in Figs. 6(a)–6(c) presents the favored island shapes as a function of the island volume V and the elastic relaxation energy density ρ_w. For very negative values of $\Delta\gamma$ only elongated islands (hut clusters and wires) form in the investigated parameter range [Fig. 6(a)]. As $\Delta\gamma$ increases, the pyramidal shape appears at higher values of ρ_w due to the enhanced relevance of shape related elastic relaxation effects [Fig. 6(b)]. At even higher values of $\Delta\gamma$, pyramids dominate [Fig. 6(c)].

The shape phase diagrams indicate that the equilibrium formation of in-plane wires is restricted to negative values of the ESE $\Delta\gamma$. For positive values of $\Delta\gamma$, pyramidal islands are favored.

For nanowires with potential quantum transport applications, it is particularly important to determine the favored base width in addition to the aspect ratio B/L. Therefore, we also derived the preferred island base widths B for the investigated parameter space, and the corresponding results are presented in the right-hand columns of Figs. 4–6. The left and right columns carry equivalent information, since either B or B/L together with V is sufficient to specify the shape. One can see that once formed, the base width of the wires is essentially constant, indicating that increases in volume only lead to increased elongation without significant changes in width or height. According to Fig. 4(d), the preferred wire width is mainly determined by the edge energy Γ_p, whereas the influence of g_r and ρ_w is rather insignificant [see Figs. 5(d) and 6(d)]. On the contrary, the pyramid base width rapidly increases with the volume, due to the obvious geometrical constraint connecting its volume to its base width. Furthermore, just like the aspect ratio, the base widths of pyramidal islands are separated by first-order phase boundary lines from the other island shapes; i.e., one can notice discontinuous changes in the corresponding base widths when crossing between the pyramid and elongated island morphologies.

We find that in some regions of the parameter space [e.g., Fig. 6(b)], the equilibrium shape even in the large-volume limit corresponds to elongated islands (wires) rather than pyramids. This might seem contrary to the simple intuitive picture that for large volumes the elastic relaxation energy (volume type) contribution would always dominate over the surface and edge

energy terms. Actually, such a scaling argument is valid only for compact 3D shapes, but not for 1D wires. According to Eqs. (1)–(4), if the shape parameter b of the elongated islands scales with volume as $\tilde{V}^{-1/3}b = \text{constant}$, then neither the surface energy term nor the edge energy contribution would vanish in the large-volume limit. In this way, the negative ESE term can win over the elastic relaxation even in the large-volume limit, preferring the growth of elongated islands. Furthermore, the condition $\tilde{V}^{-1/3}b = \text{constant}$ corresponds to $B = \text{constant}$; i.e., a constant island base width is preferred for large volumes. This latter feature is in accord with the recent theoretical findings of [12] that the several nanometers long, monolithic Ge/Si nanowires grow with a constant base width of approximately 16 nm.

We also note that at sufficiently large volumes, additional steeper facets are introduced [2,3,34,35], putting those volumes outside the range of applicability of our model. Furthermore, one cannot exclude that possible kinetic effects are responsible for the formation of the monolithic in-plane nanowires observed in [12,13]. For example, strain-dependent facet nucleation and growth effects could lead to symmetry breaking and growth of elongated nanostructures [19,20].

In summary, our shape phase diagrams demonstrate the morphological richness of rectangular-based self-assembled islands expected in strained layer heteroepitaxy assuming equilibrium energetics, emerging from the elaborate interplay of the elastic, surface, and edge energy contributions. The derived phase diagrams suggest well-defined parameter ranges for which either pyramids, huts, or wires are preferred to form. Our investigations also confirm that the presence of a negative excess surface energy is a key ingredient for wire formation in equilibrium. However, one should keep in mind the possible presence and potential importance of the above discussed kinetic effects.

ACKNOWLEDGMENTS

We are grateful to D. Scopece and F. Montalenti for providing results of Ref. [32] prior to publication. This work was financially supported by FWF (Vienna) via SFB 025: IRoN.

[1] M. Goryll, L. Vescan, K. Schmidt, S. Mesters, H. Lüth, and K. Szot, Appl. Phys. Lett. **71**, 410 (1997).
[2] G. Medeiros-Ribeiro, A. M. Bratkovski, T. I. Kamins, D. A. A. Ohlberg, and R. S. Williams, Science **279**, 353 (1998).
[3] F. M. Ross, R. M. Tromp, and M. C. Reuter, Science **286**, 1931 (1999).
[4] Y.-W. Mo, D. E. Savage, B. S. Swartzentruber, and M. G. Lagally, Phys. Rev. Lett. **65**, 1020 (1990).
[5] M. Tomitori, K. Watanabe, M. Kobayashi, and O. Nishikawa, Appl. Surf. Sci. **76–77**, 322 (1994).
[6] B. Voigtlander, M. Kawamura, N. Paul, and V. Cherepanov, J. Phys.: Condens. Matter **16**, S1535 (2004).
[7] V. A. Shchukin and D. Bimberg, Rev. Mod. Phys. **71**, 1125 (1999).
[8] G.-H. Lu and F. Liu, Phys. Rev. Lett. **94**, 176103 (2005).
[9] O. E. Shklyaev, M. J. Beck, M. Asta, M. J. Miksis, and P. W. Voorhees, Phys. Rev. Lett. **94**, 176102 (2005).
[10] Y. Chen, D. A. A. Ohlberg, and R. S. Williams, J. Appl. Phys. **91**, 3213 (2002).
[11] Y. Katayama, S. Yokoyama, T. Kobayashi, T. Meguro, and X. Zhao, Jpn. J. Appl. Phys. **47**, 5015 (2008).
[12] J. J. Zhang, G. Katsaros, F. Montalenti, D. Scopece, R. O. Rezaev, C. Mickel, B. Rellinghaus, L. Miglio, S. De Franceschi, A. Rastelli, and O. G. Schmidt, Phys. Rev. Lett. **109**, 085502 (2012).
[13] J. J. Zhang, A. Rastelli, O. G. Schmidt, D. Scopece, L. Miglio, and F. Montalenti, Appl. Phys. Lett. **103**, 083109 (2013).
[14] C. Kloeffel, M. Trif, and D. Loss, Phys. Rev. B **84**, 195314 (2011).
[15] G. Costantini, C. Manzano, R. Songmuang, O. G. Schmidt, and K. Kern, Appl. Phys. Lett. **82**, 3194 (2003).
[16] G. Costantini, A. Rastelli, C. Manzano, R. Songmuang, O. G. Schmidt, and K. Kern, Appl. Phys. Lett. **85**, 5673 (2004).
[17] G. Costantini, A. Rastelli, C. Manzano, P. Acosta-Diaz, G. Katsaros, R. Songmuang, O. G. Schmidt, H. v. Kanel, and K. Kern, J. Cryst. Growth **278**, 38 (2005).
[18] J. Tersoff and R. M. Tromp, Phys. Rev. Lett. **70**, 2782 (1993).
[19] D. E. Jesson, G. Chen, K. M. Chen, and S. J. Pennycook, Phys. Rev. Lett. **80**, 5156 (1998).
[20] M. R. McKay, J. A. Venables, and J. Drucker, Phys. Rev. Lett. **101**, 216104 (2008).
[21] G. S. Rohrer, C. L. Rohrer, and W. W. Mullins, J. Am. Ceram. Soc. **84**, 2099 (2001).
[22] J. Stangl, V. Holy, and G. Bauer, Rev. Mod. Phys. **76**, 725 (2004).
[23] D. B. Migas, S. Cereda, F. Montalenti, and L. Miglio, Surf. Sci. **556**, 121 (2004).
[24] T. Hashimoto, Y. Morikawa, and K. Terakura, Surf. Sci. **576**, 61 (2005).
[25] G.-H. Lu, M. Cuma, and F. Liu, Phys. Rev. B **72**, 125415 (2005).
[26] G. Chen, B. Sanduijav, D. Matei, G. Springholz, D. Scopece, M. J. Beck, F. Montalenti, and L. Miglio, Phys. Rev. Lett. **108**, 055503 (2012).
[27] C. J. Moore, C. M. Retford, M. J. Beck, M. Asta, M. J. Miksis, and P. W. Voorhees, Phys. Rev. Lett. **96**, 126101 (2006).
[28] P. C. Kelires and J. Tersoff, Phys. Rev. Lett. **63**, 1164 (1989).
[29] J. Tersoff, B. J. Spencer, A. Rastelli, and H. von Kanel, Phys. Rev. Lett. **89**, 196104 (2002).
[30] C. M. Retford, M. Asta, M. J. Miksis, P. W. Voorhees, and E. B. Webb III, Phys. Rev. B **75**, 075311 (2007).
[31] F. Montalenti, D. Scopece, and L. Miglio, C. R. Phys. **14**, 542 (2013).
[32] D. Scopece and F. Montalenti (unpublished).
[33] V. I. Marchenko, Zh. Eksp. Teor. Fiz. **81**, 1141 (1981) [Sov. Phys. JETP **54**, 605 (1981)].
[34] M. Brehm, H. Lichtenberger, T. Fromherz, and G. Springholz, Nano. Res. Lett. **6**, 70 (2011).
[35] I. Daruka, J. Tersoff, and A.-L. Barabási, Phys. Rev. Lett. **82**, 2753 (1999).